# Modeling the Input Power Dependency of Transceiver BER-ONSR for QoT Estimation

**Toru Mano[1,*], Yue-Kai Huang[2], Giacomo Borraccini[2], Ezra Ip[2], Andrea D'Amico[2], Zehao Wang[3], Hideki Nishizawa[1], Gil Zussman[4], Tingjun Chen[3], Ting Wang[2], Koji Asahi[5], Daniel Kilper[6], Vittorio Curri[7], Koichi Takasugi[1]**

*[1] NTT Network Innovation Labs, Kanagawa Japan, [2] NEC Labs America, Princeton, USA, [3] Duke University, Durham, NC, USA [4] Columbia University, New York, USA, [5] NEC Corporation, Chiba, Japan, [6] CONNECT Centre, Trinity College Dublin, Ireland, [7] Politecnico di Torino, Torino, Italy, [*] toru.mano@ntt.com*

**Abstract:** We propose a method to estimate the input power dependency of the transceiver BER-OSNR characteristic. Experiments using commercial transceivers show that estimation error in Q-factor is less than 0.2 dB. 

## 1. Introduction

Estimating the quality of transmission (QoT) of light paths [1] and monitoring the line system impairments or generalized signal-to-noise ratio (GSNR) [2] are vital tasks in optical network management. These two essential tasks require an understanding of the transceiver characteristic described by the relationship between pre-FEC bit error ratio (BER) or Q-factor and optical signal-to-noise ratio (OSNR) in a back-to-back setup. We call this characteristic BER-OSNR. For example, by using BER-OSNR, we can estimate Pre-FEC BER or Q-factor from GSNR estimates yielded by a tool like GNPy (Fig. 1(a)) [1]. Moreover, BER-OSNR allows us to convert monitored Pre-FEC BER at the in-service receiver to GSNR (Fig. 1(b)) [2]. These two techniques work even with open and disaggregated environments because BER and OSNR are fundamental performance parameters widely available without relying on vendor proprietary features. In both cases, accurate estimation and monitoring require the accurate determination of the transceiver BER-OSNR [3].

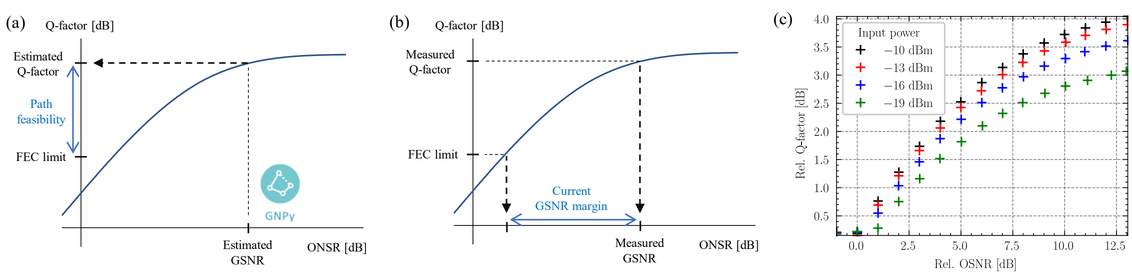


Fig. 1. (a) QoT Estimation (b) GSNR monitoring (c) Input power dependency

However, BER-OSNR is sensitive to the input power to the receiver (Fig. 1(c)). Thus, accurate QoT estimation and GSNR monitoring require us to estimate how the input power impacts the BER-OSNR. This is because the input power used in measuring BER-OSNR may differ from that of QoT estimation or GSNR monitoring. BER-OSNR represents how the transceiver impacts signal quality, and existing studies [3–6] show that, as the amplifier's amplified spontaneous emission (ASE) noise and nonlinear interference (NLI) noise can be modeled as additive Gaussian noise [1], signal degradation by transceiver can be modeled as additive Gaussian noise. [4] proposed a BER-OSNR model that treats ASE, NLI, and transceiver noises as individual Gaussian noise. [6] validated the model for modern commercial transceivers capable of higher baud rates and modulation formats and showed that the model has good accuracy, showing a modeling error of less than 0.1 dB. However, existing studies implicitly assume that the input power is always constant and thus do not consider the input power dependency of BER-OSNR.

We propose a BER-OSNR model that includes an input power penalty term to estimate the input power dependency of BER-OSNR; the key assumption is that the dominant input power penalty stems from the shot noise of the receiver photodetectors. We validate the proposed model using multiple commercial transceivers with different modulation formats, and the resulting modeling error is less than 0.04 dB. Using the proposed model, we estimate the input power dependency of BER-OSNR of commercial transceivers and find that the estimation error is less than 0.14 dB.

## 2. BER-OSNR Model with the Input Power Dependency Term

We extend the existing BER-OSNR model [4, 6] so that it can take account of input power dependency,

$$\mathrm{BER} = \Psi(\mathrm{SNR}), \quad \mathrm{SNR}^{-1} = \mathrm{SNR_{ASE}}^{-1} + \mathrm{SNR_{NLI}}^{-1} + \mathrm{SNR_{TRX}}^{-1}, \quad \mathrm{SNR_{ASE}} = \mathrm{OSNR}\frac{\Delta f}{R_s \xi} \tag{1}$$

where the function $\Psi$ is mathematically determined from the modulation format and symbol mapping [8]; e.g., $\Psi(x) = \frac{1}{2}\,\mathrm{erfc}\left(\sqrt{x/2}\right)$ for DP-QPSK, $\Psi(x) = \frac{2}{3}\,\mathrm{erfc}\left(\sqrt{\frac{3}{14}x}\right)$ for DP-8QAM, $\Psi(x) = \frac{3}{8}\,\mathrm{erfc}\left(\sqrt{x/10}\right)$ for DP-16QAM. $\mathrm{SNR_{ASE}}$ is the signal-to-noise ratio (SNR) of ASE noise, $\mathrm{SNR_{NLI}}$ is the SNR of NLI noise, $\mathrm{SNR_{TRX}}$ is the SNR of the transceiver noise attributed to the transceiver impairments, $\Delta f$ is the OSNR measuring bandwidth, which is usually 12.5 GHz, $R_s$ is the signal baud rate, and $\xi$ represents the deviations of the receiver filter from the ideal matched filter.

We assume that the dominant input power dependency stems from the shot noise of the photodetectors in the receiver. A digital coherent receiver consists of a local oscillator (LO), polarization beam splitter (PBS), beam splitter (BS), 90 optical hybrids, balanced photodetectors (BPD), transimpedance amplifier (TIA), analog-to-digital converter (ADC), and digital signal processor (DSP) (Fig. 2(a)). The SNR of the electrical output current from BPD, $\mathrm{SNR}_i$, can be represented as follows [7]

$$\mathrm{SNR}_i = \frac{R^2 S_{\mathrm{in}} S_{\mathrm{LO}}/2}{q\,(R(P_{\mathrm{in}} + P_{\mathrm{LO}}) + 4I_d)\,B + 4k_B T B/R_L + R^2(N_{\mathrm{in}} S_{\mathrm{LO}} + P_{\mathrm{in}} N_{\mathrm{LO}})/2} \tag{2}$$

where $R$ is the BPD responsivity, $S_{\mathrm{in}}$ and $S_{\mathrm{LO}}$ are the input and LO signal powers, $N_{\mathrm{in}}$ and $N_{\mathrm{LO}}$ are the input and LO noise powers, $P_{\mathrm{in}}$ and $P_{\mathrm{LO}}$ are the input and LO total powers, $q$ is the electron charge, $I_d$ is the dark current, $B$ is the effective bandwidth, $k_B$ is Boltzmann's constant, $T$ is temperature, and $R_L$ is the resistor value. The denominator's first term, $q\,(R(P_{\mathrm{in}} + P_{\mathrm{LO}}) + 4I_d)\,B$, represents the shot noise of BPD. The second term, $4k_B T B/R_L$, denotes the thermal noise. The third term, $R^2(N_{\mathrm{in}} S_{\mathrm{LO}} + P_{\mathrm{in}} N_{\mathrm{LO}})/2$, corresponds to the noise in the input and LO signals. Assuming the LO signal has sufficient power and SNR, that is, $P_{\mathrm{LO}} \gg 1$ and $P_{\mathrm{LO}} \approx S_{\mathrm{LO}}$, and the input signal has moderate SNR, $P_{\mathrm{in}} \approx S_{\mathrm{in}}$, we have $\mathrm{SNR}_i^{-1} \approx \mathrm{SNR_P}^{-1} P_{\mathrm{in}}^{-1} + \mathrm{SNR_{in}}^{-1} + \mathrm{SNR_{LO}}^{-1}$ where $\mathrm{SNR_P} = R/(2qB)$ and $\mathrm{SNR_P} P_{\mathrm{in}}$ corresponds to the signal degradation caused by the input power. Using this relationship, we extend the model (Eq (1)). Let $\mathrm{SNR}_e$ be the SNR of the noise generated after the BPD in the receiver. Then we have $\mathrm{SNR}^{-1} = \mathrm{SNR}_i^{-1} + \mathrm{SNR}_e^{-1}$. Now, we explain the relationship between $\mathrm{SNR_{in}}, \mathrm{SNR_{LO}}, \mathrm{SNR}_e$ and $\mathrm{SNR_{ASE}}, \mathrm{SNR_{NLI}}, \mathrm{SNR_{TRX}}$. $\mathrm{SNR_{TRX}}$ can be divide into the transmitter part $\mathrm{SNR_{TX}}$ and the receiver part $\mathrm{SNR_{RX}}$; $\mathrm{SNR_{TRX}^{-1}} = \mathrm{SNR_{TX}^{-1}} + \mathrm{SNR_{RX}^{-1}}$. Since $\mathrm{SNR_{in}}$ consists of the transmitter and line system impairments, we have $\mathrm{SNR_{in}^{-1}} = \mathrm{SNR_{ASE}^{-1}} + \mathrm{SNR_{NLI}^{-1}} + \mathrm{SNR_{TX}^{-1}}$. $\mathrm{SNR_{RX}}$ consists of BPD noise, LO noise and $\mathrm{SNR}_e$; $\mathrm{SNR_{RX}^{-1}} = \mathrm{SNR_P}^{-1} P_{\mathrm{in}}^{-1} + \mathrm{SNR_{LO}^{-1}} + \mathrm{SNR}_e^{-1}$. Thus, we have

$$\mathrm{SNR}^{-1} = \mathrm{SNR_{ASE}}^{-1} + \mathrm{SNR_{NLI}}^{-1} + \mathrm{SNR_{TRX'}}^{-1} + \mathrm{SNR_P}^{-1} P_{\mathrm{in}}^{-1} \tag{3}$$

where $\mathrm{SNR_{TRX'}}$ is the transceiver noise excluding the BPD noise and is defined by $\mathrm{SNR_{TRX'}^{-1}} = \mathrm{SNR_{TX}^{-1}} + \mathrm{SNR_{LO}^{-1}} + \mathrm{SNR}_e^{-1} = \mathrm{SNR_{TRX}^{-1}} - \mathrm{SNR_P}^{-1} P_{\mathrm{P}}^{-1}$. We validate and evaluate this extended BER-OSNR model in the following.

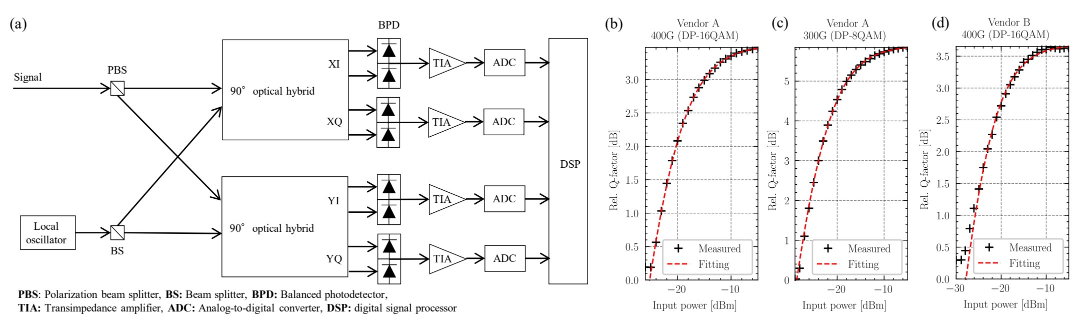


Fig. 2. (a) Digital coherent receiver (b-d) Model validation results

## 3. Experiments on Commercial Transceivers

### *3.1. Model Validation with Multiple Transceivers and Modulation Formats*

We validated the proposed model using multiple transceivers with different modulation formats by evaluating the modeling error. We measured Q-factors by changing the input power at the receiver in a back-to-back setup configuration.

We calculated the two model parameters, $\left(\mathrm{SNR}_{\mathrm{ASE}}^{-1}+\mathrm{SNR}_{\mathrm{TRX}'}^{-1}\right)^{-1}$ and $\mathrm{SNR}_{\mathrm{P}}$, via least-square fitting and computed the modeling error as RMSE in Q-factor. We set a variable optical attenuator before the receiver to change the input power. We read pre-FEC BER and input power from the receiver performance counters and determined the Q-factor as $Q = 2\mathrm{erfc}^{-1}\left(2\mathrm{BER}\right)^{2}$. During the measurements, we measured OSNR with an optical spectrum analyzer, keeping it constant at 30 dB. Note that we ignore $\mathrm{SNR}_{\mathrm{NLI}}$ due to the very short propagation distance and absence of other channels.

We tested two commercial OpenROADM-compliant CFP2-DCO modules from vendor A and another two from vendor B (we mask the vendor names for confidentiality). Vendor A's modules used OpenROADM 400G (DP-16QAM 63.1GBd) and OpenROADM 300G (DP-8QAM 63.1GBd), while vendor B's modules used OpenROADM 400G (DP-16QAM 63.1GBd). Fig. 2(b-d) show three out of the six results. The model curves (dashed lines) fit the measured values (plus points) well. The remaining three cases also showed similar results. In all six cases, RMSEs in Q-factor were less than 0.04 dB. Note that we intentionally omitted $\mathrm{SNR}_{\mathrm{in}}$ and the absolute value of Q-factor to obscure transceiver performance and ensure vendor confidentiality.

### 3.2. *Estimation Accuracy of the Input Power Dependency of BER-OSNR*

We estimated the input power dependency of BER-OSNR using the proposed model. First, we computed $\mathrm{SNR}_{\mathrm{TRX}'}$ and $\xi$ as in [6] from the measured BER-OSNR data at input power of -7 dBm and calculated $\mathrm{SNR}_{\mathrm{P}}$ as in Section 3.1. Next, using these parameters and the proposed model, we estimated BER-OSNR for the input power of -10 dBm, -13 dBm, -16 dBm, and -19 dBm. Then, we compared measured and estimated BER-OSNR for each input power. We used the same transceiver modules and operational modes as in Section 3.1.

Fig. 3 shows three out of six comparison results. The estimated BER-OSNR curves (dotted lines) agree well with the measured BER-OSNR values (plus points). The remaining three cases also showed similar results. In all six cases, RMSEs in Q-factor were less than 0.14 dB. Here, we also omitted the model parameter values, $\mathrm{SNR}_{\mathrm{TRX}'}$, $\xi$ and $\mathrm{SNR}_{\mathrm{P}}$, and the absolute values of Q-factor and OSNR to obscure transceiver performance and ensure vendor confidentiality. However, for the same vendor, the parameters did not vary significantly, showing a maximum variation of 0.8 dB. Our results imply that once we measure the BER-OSNR and the relationship between input power and Q-factor, we can accurately estimate the input power dependency of BER-OSNR and improve the accuracy of QoT estimation and GSNR monitoring.

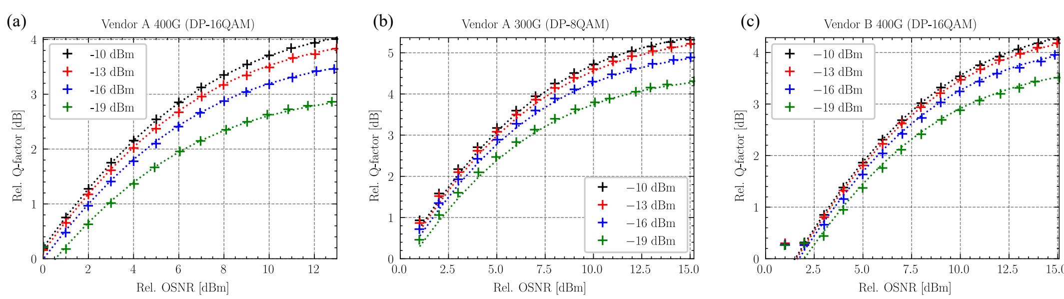


Fig. 3. Estimated (dotted lines) and measured (plus points) BER-OSNR: (a) Vendor A 400G, (b) Vendor A 300G, (c) Vendor B 400G.

## 4. Conclusion

We proposed a BER-OSNR model that considers the input power dependency and validated it using commercial transceivers; the modeling error in Q-factor was less than 0.04 dB. Another experiment demonstrated that the proposed model accurately estimated the input power dependency of BER-OSNR. The estimation error of commercial transceivers was less than 0.14 dB. Our results imply that the proposed model will be one of the critical pieces for accurate QoT estimation and GSNR monitoring and will accelerate the automation of optical networking. Future work involve a more efficient extraction methodology of the modeling parameters.

## References

1. V. Curri, JOCN, 14, C92–C104, 2022.
2. K. Kaeval et al., JOCN, 13, E1–E12, 2021.
3. P. Pecci et al., Proc. SubOptic, 2019.
4. F. Vacondio et al., Optics Express, 20, 1022–1032, 2012.
5. Z. Tao et al., JLT, 40, 3163–3172, 2022.
6. T. Mano et al., Proc. ONDM, 2023.
7. G. P. Agrawal, Jhon Wiely & Sons, 2021.
8. A. Carena et al., JLT, 30, 1524–1539, 2012.